PHYSICAL REVIEW E **68**, 065605(R) (2003)

Stabilization of one-dimensional periodic waves by saturation of the nonlinear response

Yaroslav V. Kartashov,[1,2] Alexey A. Egorov,[2] Anna S. Zelenina,[2] Victor A. Vysloukh,[3] and Lluis Torner[1]
[1]*ICFO–Institut de Ciencies Fotoniques, and Department of Signal Theory and Communications, Universitat Politecnica de Catalunya, E-08034 Barcelona, Spain*
[2]*Physics Department, M. V. Lomonosov Moscow State University, 119899 Moscow, Russia*
[3]*Departamento de Fisica y Matematicas, Universidad de las Americas-Puebla, Santa Catarina Martir, 72820 Puebla, Cholula, Mexico*

(Received 15 September 2003; published 24 December 2003)

We address the properties of $(1+1)$-dimensional periodic waves in conservative saturable cubic nonlinear media and discover that cnoidal- and snoidal-type waves are completely stable within a broad range of parameters. The existence of stability bands is in sharp contrast with the previously known properties of periodic waves in self-focusing Kerr nonlinear media. We also found that in self-defocusing media instability bands occur, again in contrast to the case of Kerr media.

DOI: 10.1103/PhysRevE.68.065605 PACS number(s): 42.65.Tg, 42.65.Jx, 42.65.Wi

Stationary periodic wave structures play an important role in a number of physical models and occur in media with various nonlinearities admitting existence of spatial or temporal solitons [1–6]. Nonlinear periodic waves by their nature are closely related to the phenomena of modulational instability and turbulence development. They describe the eigenmodes of mechanical, molecular, and electrical chains, and are connected to Bloch-type waves in solid-state physics and in diffraction or dispersion managed structures. Periodic light-induced reconfigurable lattices are used for the formation of matrices of ultracold atoms and for trapping and guiding of intense optical radiation. The properties of self-sustained periodic wave structures have been extensively studied in the past in the context of Langmuir plasma waves [5,7], deep-water gravity waves [4,8], pulse trains in optical fibers [1–3,9], reconfigurable beam arrays in photorefractive crystals [6,10], matter waves in trapped Bose-Einstein condensates [11], synchronously pumped optical parametric oscillators [12], optical cavities [13], and in quadratic nonlinear media [14].

Only a few examples of *linearly stable* periodic wave patterns are known. Such stable waves arise in defocusing cubic Kerr nonlinear media [3–5,7,8,15], in systems trapped by external potentials, such as Bose-Einstein condensates in optically induced periodic traps [11], or in dissipative optical systems such as driven optical cavities [13]. Recently it was discovered that stable multicolored periodic waves are possible under suitable conditions in quadratic nonlinear media [16]. To date, this is the only known example of stable self-sustained periodic patterns in uniform conservative media supporting bright solitons.

Here we report the existence of stable cnoidal- and snoidal-type periodic wave families in conservative media with saturable Kerr-type nonlinearity. We have found stability of periodic waves in self-focusing saturable media within a broad range of parameters, as well as narrow band of instability for waves in self-defocusing medium. This is in sharp contrast with the properties of periodic waves in cubic nonlinear media that are stable in defocusing medium and unstable in focusing medium [9,15]. We show that periodic waves become stable (unstable) in focusing (defocusing) saturable medium when field intensity exceeds the certain critical level.

We consider propagation of laser radiation in a medium with saturable cubic nonlinear response that can be met for example in photorefractive crystals [6,10,17]. The evolution of dimensionless field amplitude is described by nonlinear Schrödinger equation:

$$i\frac{\partial q}{\partial \xi}=-\frac{1}{2}\frac{\partial^2 q}{\partial \eta^2}+\frac{\sigma q|q|^2}{1+S|q|^2}. \qquad (1)$$

Here transverse η and longitudinal ξ coordinates are scaled in terms of the characteristic beamwidth and diffraction length, respectively; S is the saturation parameter; $\sigma=-1$ $(+1)$ for focusing (defocusing) media. In photorefractive crystals the value of the saturation parameter can be controlled by adjusting the biasing static electric field, and the sign of nonlinearity depends on its polarity [17]. Simple estimates show that for photorefractive SBN crystal (electro-optic coefficient $r=1.8\times10^{-10}$ m/V, linear refractive index $n_0=2.33$) biased with dc static electric field $E_0\sim10^5$ V/m, for laser beams with width 10 μm at wavelength $\lambda=0.63$ μm, the value of saturation parameter is given by $S\sim0.2$, propagation distance $\xi=1$ corresponds to 2.3 mm of actual crystal length, while dimensionless amplitude $q\sim1$ corresponds to real peak intensities about 50 mW/cm^2. One should take care of the fact that in real experiments with bulk crystals periodic waves can be affected by transverse modulational instability along uniform y axis [15].

Stationary periodic solutions of Eq. (1) have the form $q(\eta,\xi)=w(\eta)\exp(ib\xi)$, where $w(\eta)=w(\eta+T)$ is the real periodic function, b is the propagation constant, and can be found only numerically. The periodic wave families are defined by two mathematical parameters, the transverse period T and the propagation constant b, at a fixed saturation parameter S. Physically b is related to the energy flow

$$U=\int_{-T/2}^{T/2}w^2(\eta)d\eta \qquad (2)$$

inside each transverse wave period. Note that if $q(\eta,\xi,S)$ is the solution of Eq. (1) then $\chi q(\chi\eta,\chi^2\xi,\chi^{-2}S)$ (here $\chi>0$ is the arbitrary scaling factor) is also a solution of this equation. Since one can use scaling transformations to get various pe-

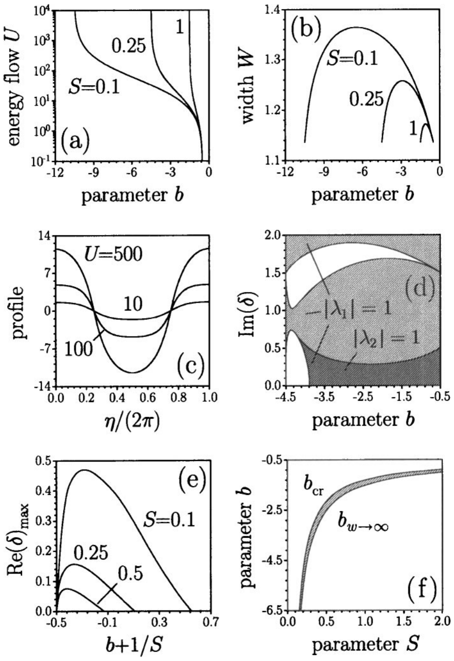

FIG. 1. Energy flow (a) and integral width (b) of sn-type wave vs propagation constant. (c) Profiles of sn waves with various energy flows at $S=0.1$. (d) Areas of existence of finite perturbations with imaginary growth rates at $S=0.25$ (shaded). (e) Maximum real part of complex growth rate vs propagation constant. (f) Areas of existence of stable and unstable (shaded) sn waves. All quantities are plotted in dimensionless units.

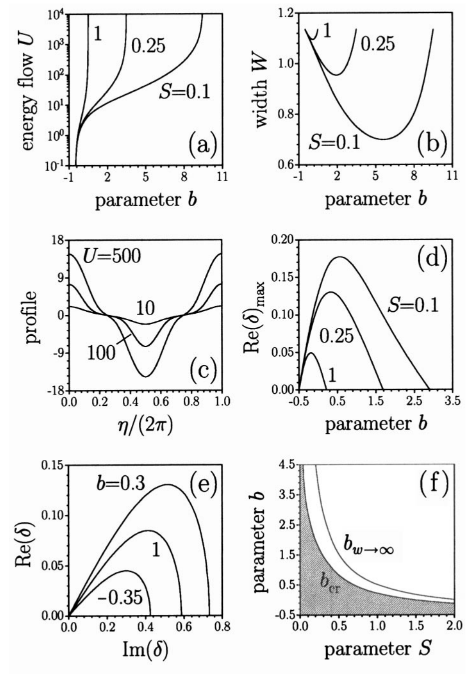

FIG. 2. Energy flow (a) and integral width (b) of cn-type wave vs propagation constant. (c) Profiles of cn waves with various energy flows at $S=0.1$. (d) Maximum real part of complex growth rate vs propagation constant. (e) Curves at the complex plane showing possible increment values for various propagation constants at $S=0.25$. (f) Areas of existence of stable and unstable (shaded) cn waves. All quantities are plotted in dimensionless units.

riodic wave families from the known ones we choose the transverse scale so that period $T=2\pi$.

The main properties of periodic wave solutions of Eq. (1) are summarized in Figs. 1(a)–1(c), 2(a)–2(c), 3(a), and 3(b). There are three types of lowest order periodic waves: *snoidal* (sn) wave in defocusing medium ($\sigma=+1$), *cnoidal* (cn) and *dnoidal* (dn) waves in focusing medium ($\sigma=-1$). We use these notations for wave types by analogy, despite the fact that exact solutions of Eq. (1) are described by Jacobi elliptic functions only in the limiting case $S\rightarrow 0$. sn- and cn-type waves periodically change their sign [Figs. 1(c) and 2(c)], whereas dn wave is always positive and contains a constant pedestal [Fig. 3(b)].

Dispersion diagrams for sn and cn waves are quite similar [see Figs. 1(a) and 2(a)]. In the limit $w\rightarrow 0$ and $w\rightarrow\infty$ both sn and cn waves are transformed into harmonic patterns. The corresponding low- and high-energy cutoffs are given by $b_{w\rightarrow 0}=-1/2$ and $b_{w\rightarrow\infty}=-1/2-\sigma/S$. The domain of existence of dn-type wave is narrowed with growth of saturation parameter [Fig. 3(a)]. Near the cutoffs the dn wave is close to plane wave. The integral width defined as

$$W=2\left(\int_{-T/4}^{T/4}w^2(\eta)\eta^2 d\eta\right)^{1/2}\left(\int_{-T/4}^{T/4}w^2(\eta)d\eta\right)^{-1/2} \quad (3)$$

reaches its maximum value for sn waves [Fig. 1(b)] and its minimum value for cn waves [Fig. 2(b)] at intermediate energy levels, which correspond to the narrowest dark holes and bright peaks (or strongest *degree of localization*) for sn and cn waves, respectively. For strong localization cn waves transform into arrays of out-of-phase bright solitons, dn wave into arrays of in-phase bright solitons, and sn wave into arrays of out-of-phase kinks, or dark solitons.

To analyze stability of periodic waves in the saturable

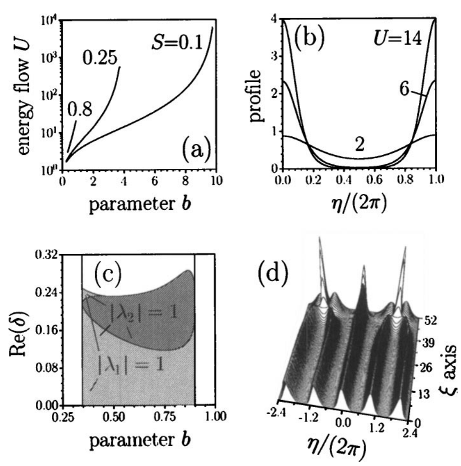

FIG. 3. (a) Energy flow of a dn-type wave vs propagation constant. (b) Profiles of dn waves with various energy flows at $S=0.1$. (c) Areas of existence of finite perturbations with real growth rates at $S=0.8$ (shaded). Vertical lines in (c) stand for cutoffs. (d) Propagation of dn-wave with $b=0.6$ and $S=0.25$ in the presence of perturbation with growth rate $\delta=0.1084$. All quantities are plotted in dimensionless units.

medium we seek for perturbed solutions of Eq. (1) in the form [15,16]

$$q(\eta,\xi)=[w(\eta)+U(\eta,\xi)+iV(\eta,\xi)]\exp(ib\xi), \qquad (4)$$

with $w(\eta)$ being the stationary solution of Eq. (1), and U and V real and imaginary parts of small perturbation, respectively. We look for exponentially growing perturbations $U(\eta,\xi)=\mathrm{Re}[u(\eta,\delta)\exp(\delta\xi)]$ and $V(\eta,\xi)=\mathrm{Re}[v(\eta,\delta)\exp(\delta\xi)]$, where δ is the complex growth rate. Substitution of Eq. (4) into Eq. (1) and linearization yields the matrix equation

$$\frac{d\Phi}{d\eta}=\mathcal{B}\Phi,\quad \mathcal{B}=\begin{pmatrix}\mathcal{O} & \mathcal{E}\\ \mathcal{N} & \mathcal{O}\end{pmatrix},$$

$$\mathcal{N}=\begin{pmatrix} 2b+2\sigma\dfrac{3w^2+Sw^4}{(1+Sw^2)^2} & 2\delta \\ -2\delta & 2b+2\sigma\dfrac{w^2+Sw^4}{(1+Sw^2)^2}\end{pmatrix} \qquad (5)$$

for the perturbation vector $\Phi(\eta)=\{u,v,du/d\eta,dv/d\eta\}^{\mathrm{T}}$, where $\mathcal{O}$ and $\mathcal{E}$ are zero and unity 2×2 matrices, respectively. The general solution of Eq. (5) can be expressed in the form $\Phi(\eta)=\mathcal{J}(\eta,\eta')\Phi(\eta')$. Here $\mathcal{J}(\eta,\eta')$ is the 4×4 Cauchy matrix, which is the solution of the initial value problem $\partial\mathcal{J}(\eta,\eta')/\partial\eta=\mathcal{B}(\eta)\mathcal{J}(\eta,\eta')$, $\mathcal{J}(\eta',\eta')=\mathcal{E}$.

The Cauchy matrix defines the matrix of translation of the perturbation eigenvector Φ on one wave period as $\mathcal{P}(\eta)=\mathcal{J}(\eta+T,\eta)$. It was rigorously proven in Refs. [15], [16] that the perturbation eigenvector $\Phi_k(\eta)$ is finite along the transverse η axis when the corresponding eigenvalue of the matrix of translation satisfies the condition $|\lambda_k|=1$ $(k=1,\ldots,4)$. This condition defines the algorithm of construction of the *areas* of existence of finite perturbations. The eigenvalues λ_k are defined by the characteristic polynomial $D(\lambda)=\det(\mathcal{P}-\lambda\mathcal{E})=\Sigma_{k=0}^{4}p_k\lambda^{4-k}=0$. The coefficients of the polynomial are given by the traces of translation matrix $T_k=\mathrm{Tr}[\mathcal{P}^k(\eta)]$. One finds that $p_0=p_4=1$, $p_1=p_3=-T_1$, and $p_2=(T_1^2-T_2)/2$. Two of the four eigenvalues λ_k can be excluded because $\lambda_k=1/\lambda_{k+2}$ $(k=1,2)$, and corresponding eigenvectors fulfill the symmetry relations $\Phi_k(\eta)=\Phi_{k+2}(-\eta)$.

First we applied the method to sn waves. We have covered a broad interval of saturation parameter $0\leq S\leq 10$ and considered perturbations with general complex growth rates. When searching for finite perturbations we scanned the whole δ plane with fine meshes (typically the step in the modulus of δ was 0.001 and the step in the phase was $\pi/1000$). For periodic patterns the areas of existence of finite perturbations have a *band structure* and one of the conditions $|\lambda_{1,2}|=1$ is fulfilled inside these bands. Figure 1(d) shows such bands for perturbations with imaginary δ. In contrast to the case of defocusing cubic medium, where sn waves are stable in the entire domain of their existence, we have found that in saturable media sn waves become *weakly unstable* when their energy flow exceeds a certain critical value (i.e., when $b\geq b_{\mathrm{cr}}$). This instability corresponds to complex

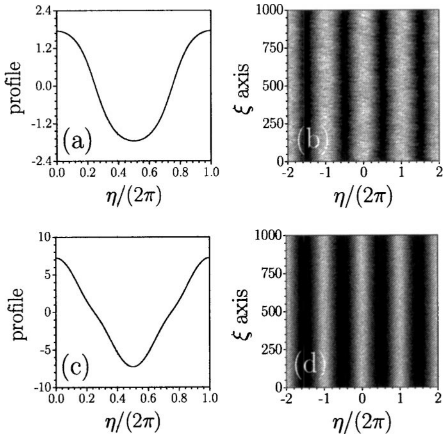

FIG. 4. (a) Profile of stationary sn wave with $b=-2$ and (b) its long-term propagation in the presence of white input noise superimposed to the stationary solution. (c) Profile of stationary cn wave with $b=3$ and (d) its long-term propagation in the presence of noise. Saturation parameter $S=0.25$. Noise variance $\sigma^2=0.01$. All quantities are plotted in dimensionless units.

growth rates and, hence, is of the oscillatory type. The maximum real part of the complex growth rate versus propagation constant is shown in Fig. 1(e). The oscillatory instability of the sn waves occurs in the narrow band of propagation constants near the high-energy cutoff. The domains of existence of stable $(b_{\mathrm{cr}}<b\leq -1/2)$ and unstable $(b_{w\to\infty}\leq b\leq b_{\mathrm{cr}})$ sn waves are shown in Fig. 1(f). Notice that for $S\to 0$ the width of the instability band vanishes, a result that is in agreement with the known results for sn waves in defocusing cubic medium.

Next we consider the case of cn waves. In Kerr media such waves suffer from oscillatory instabilities in their entire domain of existence. In contrast, the central result of the present paper is that cn waves in focusing saturable media become *linearly stable* when their energy flow exceeds a certain critical level [Figs. 2(d) and 2(f)]. This is consistent with the strong stabilizing action of saturation of nonlinear response on propagation of self-sustained nonlinear waves, dramatically illustrated by the stabilization of bell-shaped bright soliton in bulk media [18]. The effect reported here follows the stabilization of multicolor cn waves discovered recently in quadratic nonlinear media [16], and is the second example of stable periodic pattern in uniform media supporting bright solitons.

The oscillatory-type instability found for cn waves in saturable media occurs for the band of propagation constants near the low-energy cutoff, i.e., for $-1/2\leq b\leq b_{\mathrm{cr}}$. The maximal real part of complex growth rate versus propagation constant is shown in Fig. 2(d). Notice that real parts of growth rates quickly decrease with increase of saturation parameter. This means that even periodic waves from the unstable region can be observed at high saturation levels because their typical decay length would exceed any experimentally feasible crystal length. At fixed S and propagation constant, the complex growth rates for the waves from unstable region form the *curves* in the complex plane $(\mathrm{Re}(\delta),\mathrm{Im}(\delta))$ shown in Fig. 2(e). Areas of existence of stable (for $b_{cr}<b\leqslant b_{w\to\infty}$) and unstable (for $-1/2\leqslant b\leqslant b_{cr}$) cn waves at (S,b) plane are shown in Fig. 2(f). The width of the stability band increases with decrease of saturation parameter. In the limit $S\to 0$ results are in full agreement with those for unstable cn waves in cubic media.

For the sake of completeness, we have studied the case of dn-type waves and found that they suffer from exponentially growing instabilities. The typical structure of areas for finite perturbations with real growth rates is shown in Fig. 3(c). Notice that the instability of dn wave typically manifests itself in fusion of neighboring peaks [Fig. 3(d)].

To confirm the results of the linear stability analysis and to elucidate its actual impact in the long-term evolution of the periodic waves, we have also integrated Eq. (1) numerically with input conditions $q(\eta,\xi=0)=w(\eta)[1+\rho(\eta)]G(\eta)$, where $w(\eta)$ is the profile of the stationary wave, $\rho(\eta)$ is a Gaussian noise with the variance σ^2, and $G(\eta)$ is a broad Gaussian envelope imposed on the infinite periodic pattern. Results of numerical integration are in full agreement with results of linear stability analysis. For example, Figs. 4(a)–4(d) illustrate the stable propagation of perturbed snoidal and cnoidal waves with parameters belonging to stability bands. The periodic waves maintain their input structure over several thousand units, corresponding to actual physical distances, more than 2 m in typical photorefractive crystals.

In conclusion, the linear stability analysis of periodic waves in conservative saturable cubic nonlinear media, carried with a powerful mathematical formalism, has revealed the existence of *completely stable* patterns of both snoidal and cnoidal types. Such result is in contrast to the instability of periodic waves in self-focusing Kerr media. The existence of stable periodic wave arrays is thus of fundamental importance. It might find applications in the formation of reconfigurable light-induced periodic waveguide arrays in future photonic circuits.

ACKNOWLEDGMENTS

Y.V.K. and L.T. acknowledge support by the Generalitat de Catalonya and by the Spanish Government under Contract No. TIC2000-1010.

[1] N. N. Akhmediev and A. Ankiewicz, *Solitons* (Chapman-Hall, London, 1997). Yu. S. Kivshar and G. Agrawal, *Optical Solitons* (Academic, New York, 2003).

[2] A. M. Kamchatnov, *Nonlinear Periodic Waves and their Modulations* (Kluwer Academic, Dordrecht, 2000).

[3] E. Infeld and R. Rowlands, *Nonlinear Waves, Solitons and Chaos* (Cambridge University Press, Cambridge, 1990).

[4] H. C. Yuen and B. M. Lake, *Nonlinear Dynamics of Deep-Water Gravity Waves* (Academic, New York, 1982).

[5] E. A. Kuznetsov *et al.*, Phys. Rep. **142**, 103 (1986).

[6] J. W. Fleischer *et al.*, Nature (London) **422**, 147 (2003).

[7] S. E. Fil'chenkov *et al.*, Sov. J. Plasma Phys. **13**, 554 (1987); V. P. Pavlenko and V. I. Petviashvili, *ibid.* **8**, 117 (1982).

[8] D. U. Martin *et al.*, Wave Motion **2**, 215 (1980).

[9] V. P. Kudashev and A. B. Mikhailovsky, Sov. Phys. JETP **63**, 972 (1986); N. N. Akhmediev *et al.*, Teor. Mat. Fiz. **72**, 183 (1987); M. Florjanczyk and R. Tremblay, Phys. Lett. A **141**, 34 (1989); V. M. Petnikova *et al.*, Phys. Rev. E **60**, 1 (1999); F. T. Hioe, Phys. Rev. Lett. **82**, 1152 (1999).

[10] V. A. Aleshkevich *et al.*, Quantum Electron. **31**, 257 (2001).

[11] J. C. Bronski *et al.*, Phys. Rev. Lett. **86**, 1402 (2001); Phys. Rev. E **63**, 036612 (2001); **64**, 056615 (2001); P. J. Y. Louis *et al.*, Phys. Rev. A **67**, 013602 (2003); N. K. Efremidis and D. N. Christodoulides, *ibid.* **67**, 063608 (2003).

[12] A. Ankiewicz *et al.*, Phys. Lett. A **308**, 397 (2003); K.-I. Maruno *et al.*, Physica D **176**, 44 (2003).

[13] G. K. Harkness *et al.*, Phys. Rev. E **66**, 046605 (2002); S. Longhi, Phys. Rev. A **59**, 4021 (1999).

[14] P. Ferro and S. Trillo, Phys. Rev. E **51**, 4994 (1995); D. F. Parker, J. Opt. Soc. Am. B **15**, 1061 (1998); S. Lafortune *et al.*, Phys. Rev. E **58**, 2518 (1998); Y. V. Kartashov *et al.*, *ibid.* **67**, 066612 (2003).

[15] Y. V. Kartashov *et al.*, Phys. Rev. E **67**, 036613 (2003); J. Opt. Soc. Am. B **20**, 1273 (2003); Phys. Rev. E **67**, 066605 (2003).

[16] Y. V. Kartashov *et al.*, Phys. Rev. Lett. (to be published); Y. V. Kartashov *et al.*, Phys. Rev. E **68**, 046609 (2003).

[17] G. Duree *et al.*, Phys. Rev. Lett. **71**, 533 (1993); M. Segev *et al.*, Opt. Photonics News **4**, 8 (1993); Phys. Rev. Lett. **73**, 3211 (1994); G. Duree *et al.*, Opt. Lett. **19**, 1195 (1994); M. Shih *et al.*, *ibid.* **21**, 324 (1996); G. I. Stegeman and M. Segev, Science **286**, 1518 (1999).

[18] M. G. Vakhitov and A. A. Kolokolov, Radiophys. Quantum Electron. **16**, 783 (1973).